

# LISA VI

---

## DJIN : Detection in Journals of Identifiers and Names

*by Soizick Lesteven*

*C. Bonnin, S. Derrière, P. Dubois, F. Genova, A. Oberto, F. Ochsenbein, S. Borde, G. Chassagnard,  
M. Brouty, C. Bruneau, C. Brunet, H. Claude, A. Eisele, S. Laloë, M. Neuville, E. Perret, P. Vannier,  
P. Vonflie, M.-J. Wagner and F. Woelfel*

*Pune 2010*



# Permanent evolution for updating



1972



Punch card



CSI



LISAVI

- PUNE 2010 -

Soizick Lesteven



# Permanent evolution for updating



1972



Punch card



CSI

1980



alpha 20 → vt100



SIMBAD2



# Permanent evolution for updating



1972



Punch card



CSI

1980



alpha 20 → vt100



SIMBAD2

1990



X terminal → PC



SIMBAD3



# Permanent evolution for updating



Online articles

1972



Punch card



CSI

1980



alpha 20 → vt100



SIMBAD2

1990



X terminal → PC



SIMBAD3

# Permanent evolution for updating

SIMBAD

Online articles

1972



Punch card



CSI

1980



alpha 20 → vt100



SIMBAD2

1990



X terminal → PC



SIMBAD3

2006

SIMBAD4

# The last one : DJIN



2008

★ Annotated PDF with direct links to SIMBAD

★ Revolutionary tool for the information scientists who update SIMBAD

★ Development began during the VO-TECH project.

annot.pdf - Adobe Reader

File Edit View Document Tools Window Help

annot.pdf

685 (1 of 14) 80.99%

Bookmarks

- B1950
- B3
- B3i
- C2
- CM 67
- DDO 9
- Fred
- H2
- H $\alpha$  2-10
- IC 342
- J2000
- Leo Triplet
- M 51
- M 82
- M 83
- Maffei 2
- N 278
- N 3628
- N 660
- NGC 1068
- NGC 2146
- NGC 253
- NGC 278
- NGC 3079
- NGC 3623
- NGC 3627
- NGC 3628
- NGC 4627
- NGC 4631
- NGC 4632
- NGC 4656
- NGC 4666
- NGC 4668
- NGC 4826
- NGC 4945
- NGC 5194
- NGC 5236
- NGC 628 Group
- NGC 660
- NGC 6946
- NGC 7331
- NGC 7469
- OVRO 4
- RA 114

A&A 506, 689–702 (2009)  
DOI: 10.1051/0004-6361/200811586  
© ESO 2009

**Astronomy  
& Astrophysics**

## Cl and CO in nearby galaxy centers

### The star-burst galaxies NGC 278, NGC 660, NGC 3628, NGC 4631, and NGC 4666

<http://simbad.u-strasbg.fr/simbad/sim-id?proc=full&simid=NGC+4631>

Sterrewacht Leiden, Leiden University, PO Box 9513, 2300 RA Leiden, The Netherlands  
e-mail: 11rfa1@strw.leidenuniv.nl

Received 23 December 2008 / Accepted 15 August 2009

#### ABSTRACT

**Aim.** We study the physical properties and mass of molecular gas in the central regions of galaxies with active nuclei.  
**Methods.** Maps and measurements of the  $J=1-0$ ,  $J=2-1$ ,  $J=3-2$ ,  $J=4-3$   $^{12}\text{CO}$ , the  $J=1-0$ ,  $J=2-1$  and  $J=3-2$   $^{13}\text{CO}$  lines in the central armistice squared of NGC 278, NGC 660, NGC 3628, NGC 4631, and NGC 4666, as well as 492 GHz [CII] maps in three of these are used to model the molecular gas.  
**Results.** All five objects contain bright CO emission in the central region. Clear central concentrations were found in NGC 660, NGC 3628, and NGC 4666, but not in the weakest CO emitters NGC 278 and NGC 4631. In all cases, the observed lines could be modeled only with at least two distinct gas components. The physical conditions of the molecular gas is found to differ from galaxy to galaxy. Relatively ionized (density 100–1000  $\text{cm}^{-3}$ ) and high kinetic temperature (100–150 K) gas occur in all galaxies, except perhaps NGC 3628, mixed with cooler (10–50 K) and denser ( $3.3-1.0 \times 10^4 \text{ cm}^{-3}$ ) gas. The CO-to- $\text{H}_2$  conversion factor  $X$  is typically an order of magnitude less than the “standard” value in the Solar Neighborhood in all galaxy centers. The molecular gas is constrained within radii between 0.6 and 1.5 kpc from the nuclei. Within these radii,  $\text{H}_2$  masses are typically  $0.6-1.5 \times 10^6 M_{\odot}$ , which corresponds to no more than a few per cent of the dynamical mass in the same region.

**Key words.** galaxies: ISM – submillimeter – galaxies: nuclei – galaxies: starburst – galaxies: spiral

#### 1. Introduction

Molecular hydrogen ( $\text{H}_2$ ) is a major constituent of the interstellar medium in late-type galaxies. Dense clouds of molecular gas are commonly found in the arms of spiral galaxies, but are frequently also concentrated in the inner few kiloparsecs. These concentrations of gas play an important role in the evolution of galaxy centers. They provide the material for the occurrence of inner galaxy star-bursts and the accretion of super massive black holes in the nucleus. It is therefore important to determine their characteristics (density, temperature, excitation) and especially their mass but molecular hydrogen itself is very hard to observe directly. Instead, its properties are usually inferred from observations of tracer elements, notably the relatively abundant and easily excited CO molecule. Unfortunately, the CO emitting gas is not in LTE, and the most commonly observed  $^{12}\text{CO}$  lines are optically thick. We have to observe CO in various transitions to obtain reliable physical results and also in an optically thin isotopes such as  $^{13}\text{CO}$  in order to break the temperature-density degeneracy that plagues  $^{12}\text{CO}$  intensities. The measured molecular (and atomic) line intensities are the essential input for modeling of the physical state of the gas.

We have observed a sample of nearby spiral galaxy centers in various CO transitions and in the 492 GHz  $^{13}\text{CO}$ ,  $^{13}\text{CII}$  transition. These galaxies were selected to be bright at infrared wavelengths, and more specifically to have IRAS flux densities  $f_{12\mu\text{m}} \geq 1.0 \text{ Jy}$ . The results for a dozen galaxies from this sample have already been published. These are NGC 253 (Israel et al. 1995), NGC 7331 (Israel & Baas 1990), NGC 5942, and M 83 = NGC 3326 (Israel & Baas 2001 – Paper I, see also Israel & Baas 2003 – Paper II).

#### 2. Sample galaxies

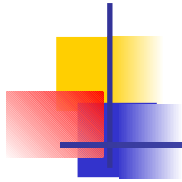
2.1. NGC 278 = DDO 9

This is an isolated, relatively small and almost face-on galaxy with a bright nucleus and multiple, spiral arms. Its optical size is about 2” corresponding to a diameter of 7 kpc. However, in

M 51 = NGC 5194 (Israel et al. 2006 – Paper III), NGC 1068, NGC 2146, NGC 3079, NGC 4826, and NGC 7462 (Israel 2009 – Paper IV). In this paper, we present the results obtained for five bright galaxies undergoing intense star formation (star-burst) in their inner parts. We have summarized basic observational parameters of these galaxies in Table 1.

Although the appearance of all five galaxies in this paper is completely dominated by a central star-burst, NGC 4666 and perhaps NGC 3628 also contain a very modest AGN. NGC 4666 shows clear evidence for a recent merger event, and NGC 278 may also have experienced a recent (minor) merger. The other three galaxies, NGC 3628, NGC 4631, and NGC 4666, are somewhat closer at 8 Mpc, and one (NGC 4666) somewhat more distant at 23 Mpc. Thus, our best angular resolutions of  $10''-14''$  correspond to linear resolutions of typically 600–850 pc. This is not sufficient to reveal appreciable structural detail in the central CO distributions; millimeter array observations are required for that. However, the multi-transition observations of  $^{12}\text{CO}$  and  $^{13}\text{CO}$  presented here allow us to characterize the overall physical condition of the central molecular gas in ways not possible otherwise.

Article published by EDP Sciences



# Context

---

- ★ Significant and continuous increase in the volume of bibliographic data to enter in SIMBAD
- ★ MNRAS :
  - 2000 : 937 references and 9267 pages
  - 2009 : 1815 references and 19916 pages
- ApJ :
  - 2000 : 2388 references and 24894 pages
  - 2009 : 3590 references and 40869 pages
- ★ SIMBAD contains on 2010.02.09 :
  - 4,750,234 objects
  - 13,521,030 identifiers
  - 238,603 bibliographic references
  - 6,896,142 citations of objects in papers

2009A&A...508..371H

Raw PDF document



Dictionary of nomenclature

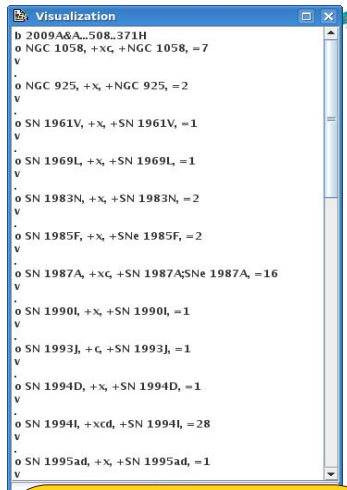
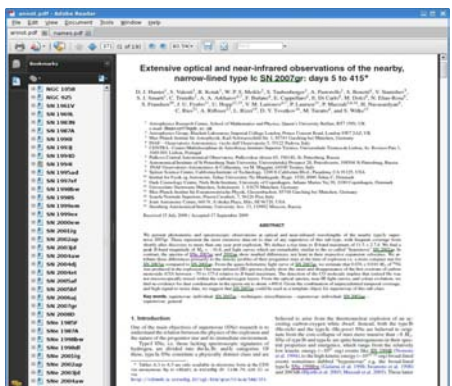
Detection of astronomical objects



Extraction of the text



Working document



Update



Annotated document

Identifiers list



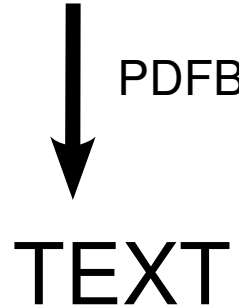
# Text Extraction : from PDF to TEXT

---

- ★ Extract from several formats (following the different publishers)
- ★ Detect the column (when 2-column text), reassemble words and paragraphs
- ★ Detect type of text (title, abstract, legend, tables, footnotes, ...)
- ★ Recognize special characters ( $\alpha$ , fi, ...)
- ★ Deal with images, figures, tables, ...



PDFBox



# Identifiers as written in the literature

★ All kind of acronyms : HD 123, USNO-B1.01484-00003998,  
Ford M 31 325, [SK98] Center 18

★ Variables stars : SU Ursa Majoris,  $\beta$  Peg, 10 And, ...

★ NAMES : ed. While Vega does have a circumstellar shell, the  
(e.g., Cox 2000).

★ With graphical symbols : ( $\alpha$ - $\omega$  + - . \*)

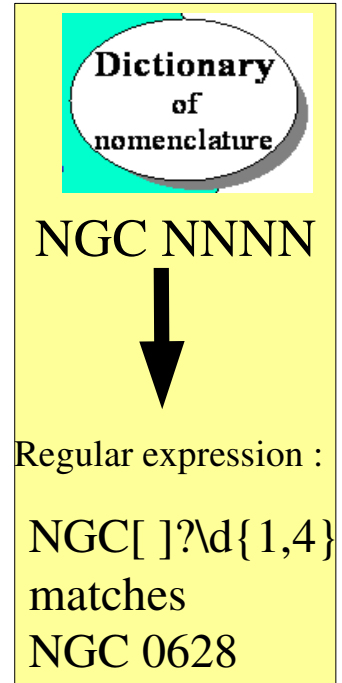
★ Lists separated by a coma :

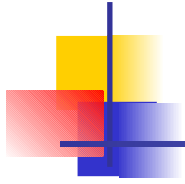
maps: IC342, NGC 0628, 99, 3521, 537 and 4414. In these cases, the relative angular sizes of the beam and galaxy, the inclination, or the CO distribution likely have contributed to spa-

★ Lists in tables, ...

# Dictionary of Nomenclature

- ★ Object Identifiers have been collected and published in Dictionaries of Nomenclature of Celestial Objects, maintained at CDS. This Dictionary which is updated on a regular basis provides full references and usages (formats) about 19.500 different acronyms.
- ★ Translate the astronomical object nomenclature format into a regular expression ← *improvement of the dictionary*
- ★ Find these regular expressions in the text → *object names*
- ★ Check their existence in SIMBAD, display their main object's type according SIMBAD, display all possible object's names according to the Dictionary and rank them according to the usage





# *A few features*

---

Why DJIN is really a very helpful tool  
for updating SIMBAD ?

Journal: A&amp;A Volume: 508 Bibcode: 2009A&amp;A...508..371H



62 object names (412)

- 6-10 (1)
- C I (11)
- C II (3)
- DD-3 (1)
- GN-2007B (1)
- GN-2008B (1)
- H-K (1)
- I 10830 (1)
- I 15025 (1)
- I 3888 (1)
- I 5875 (1)
- I 5876 (1)
- I 5890 (1)
- I 5896 (1)
- I 6300 (1)
- I 7774 (4)
- II 6355 (2)
- NGC 1058 (7)
- NGC 925 (2)
- P Cygni (5)
- Schaefer 1999 (1)
- Sep (4)
- SN 1961V (1)
- SN 1969L (1)
- SN 1983N (2)
- SN 1987A (14)
- SN 1990I (1)
- SN 1993J (1)
- SN 1994D (1)
- SN 1994I (27)
- SN 1995ad (1)
- SN 1997ef (1)
- SN 1998bw (10)
- SN 1998S (2)
- SN 1999em (2)
- SN 1999ex (5)
- SN 2000ew (3)
- SN 2001ig (1)
- SN 2002ap (49)
- SN 2003jd (6)
- SN 2004aw (15)
- SN 2004dj (4)
- SN 2004et (2)
- SN 2005af (1)

## c(c) ESO 2009Astrophysics Extensive optical and near-infrared observations of the nearby, narrow-lined type Ic **SN 2007gr**: days 5 to 415\*

### Text

D. J. Hunter, S. Valenti, R. Kotak, W. P. S. Meikle, S. Taubenberger, A. Pastorello, S. Benetti, V. Stanishev, S. J. Smartt, C. Trundle, A. A. Arkharov, F. Bufano, E. Cappellaro, E. Di Carlo, M. Dolci, N. Elias-Rosa, S. Frandsen, J. U. Fynbo, U. Hopp, V. M. Larionov, P. Laursen, P. Mazzali, H. Navasardyan, C. Rios, A. Riffeser, L. Rizzi, D. Y. Tsvetkov, M. Turatto, and S. Wilke

### 1. Introduction

#### Text

One of the main objectives of supernovae (SNe) research is to understand the relation between the physics of the explosion and the nature of the progenitor star and its immediate environment.

Type I SNe, i.e. those lacking spectroscopic signatures of hydrogen, are divided into the Ia, Ib, and Ic categories. Of these, type Ia SNe constitute a physically distinct class and are believed to arise from the thermonuclear explosion of an accreting carbon-oxygen white dwarf. Instead, both the type Ib (He-rich) and the type Ic (He-poor) SNe are believed to originate from the core-collapse of stars more massive than  $\sim 8 M_{\odot}$ .

SNe of type Ib and type Ic are quite heterogeneous in their spectral properties and energetics, which range from the relatively low kinetic energy ( $\sim 10$  erg) events like **SN 1994I** (Nomoto et al. 1994), to the high kinetic energy ( $\sim 10$  erg) broad-lined events sometimes dubbed "hypernovae" e.g. the broad-lined type Ic **SN 1998bw** (Galama et al. 1998; Iwamoto et al. 1998) and 2003dh (Hjorth et al. 2003; Mazzali et al. 2003). These latter SNe have been associated with long-duration gamma-ray bursts (GRBs) (see Woosley & Bloom 2006, for a recent review).

At present, there is no consensus regarding the differences between the progenitors that produce type Ib and Ic SNe.

However, it is generally accepted that Wolf-Rayet stars are the most promising candidates as these have shed their outer layer of H, as well as varying amounts of their He layer (Wheeler & Livrea 1985). The H and He layers are primarily shed through strong stellar winds, resulting in WC and WO stars (i.e.

carbon and oxygen dominated, respectively). The same mass-loss mechanism may likewise only remove the H layers so that the potential progenitors of type Ib **SN 1994I**, i.e. WN stars (nitrogen dominating over carbon) exhibit the products of core-H burning. Alternatively, the outermost layers may be stripped off by a companion star (Podsiadlowski et al. 1992) with the degree of envelope-stripping depending on the configuration of the binary system (Pols & Nomoto 1997).

The distinction between type Ib and type Ic SNe is historical, and challenged by the idea that He may be present in both types.

The detection of spectral features due to He in type Ib SNe might simply imply that the element is high in abundance and/or a sufficient quantity of radioactive nickel is mixed into the He layer, providing an excitation source (Wheeler et al. 1987; Shigeyama et al. 1990; Hachisu et al. 1991). The converse may be true for type Ic SNe explaining the non-detection of optical He I lines in type Ic spectra (Nomoto et al. 1990; Hachisu et al. 1991). Most important, no type Ic SN has yet displayed the isolated near-IR He line at 2.058  $\mu\text{m}$  to a strength comparable to those detected in type Ib SNe.

Consequently, it is possible that a continuous degree of He abundances and/or excitation exists from type Ib to Ic SNe, making the

| File                                | Name                                | Identifier | Search         | Configuration | Help |
|-------------------------------------|-------------------------------------|------------|----------------|---------------|------|
|                                     | Check found names                   |            | Ctrl-N         |               |      |
|                                     | Request SIMBAD                      |            |                |               |      |
|                                     | Request bibcode in SIMBAD           |            |                |               |      |
|                                     | Search already entered names        |            |                |               |      |
|                                     | Delete a name                       |            | Supprimer      |               |      |
|                                     | Mark selected names as done         |            | Ctrl-D         |               |      |
|                                     | Mark selected names as undetermined |            | Ctrl-Supprimer |               |      |
|                                     | View name list                      |            |                |               |      |
| <input type="checkbox"/>            | Display rejected names...           |            |                |               |      |
| <input type="checkbox"/>            | Display undetermined names...       |            |                |               |      |
| <input checked="" type="checkbox"/> | Display done names...               |            |                |               |      |

Bibcode : 2009A&amp;A...508..371H



# astrophysics Extensive optical and near-infrared observations of a broad-lined type Ic **SN 2007gr**: days 5 to 415\*

W. P. S. Meikle, S. Taubenberger, A. Pastorello, S. Benetti, V. Stanishev, S. J. Smartt, C. Trundle, A. A. S. Fransson, E. Di Carlo, M. Dolci, N. Elias-Rosa, S. Frandsen, J. U. Fynbo, U. Hopp, V. M. Larionov, P. Laursen, P. A. Mazzali, A. Riffeser, L. Rizzi, D. Y. Tsvetkov, M. Turatto, and S. Wilke

## 1. Introduction

### Text

One of the main objectives of supernovae (SNe) research is to understand the relation between the physics of the explosion and the nature of the progenitor star and its immediate environment.

Type I SNe, i.e. those lacking spectroscopic signatures of hydrogen, are divided into the Ia, Ib, and Ic categories. Of these, type Ia SNe constitute a physically distinct class and are believed to arise from the thermonuclear explosion of an accreting carbon-oxygen white dwarf. Instead, both the type Ib (He-rich) and the type Ic (He-poor) SNe are believed to originate from the core-collapse of stars more massive than  $\sim 8 M_{\odot}$ .

SNe of type Ib and type Ic are quite heterogeneous in their spectral properties and energetics, which range from the relatively low kinetic energy ( $\sim 10$  erg) events like **SN 1994I** (Nomoto et al. 1994), to the high kinetic energy ( $\sim 10$  erg) broad-lined events sometimes dubbed "hypernovae" e.g. the broad-lined type Ic **SNe 1998bw** (Galama et al. 1998; Iwamoto et al. 1998) and 2003dh (Hjorth et al. 2003; Mazzali et al. 2003). These latter SNe have been associated with long-duration gamma-ray bursts (GRBs) (see Woosley & Bloom 2006, for a recent review).

At present, there is no consensus regarding the differences between the progenitors that produce type Ib and Ic SNe.

However, it is generally accepted that Wolf-Rayet stars are the most promising candidates as these have shed their outer layer of H, as well as varying amounts of their He layer (Wheeler & Levreault 1985). The H and He layers are primarily shed through strong stellar winds, resulting in WC and WO stars (i.e.

carbon and oxygen dominated, respectively). The same mass-loss mechanism may likewise only remove the H layers so that the potential progenitors of type Ib **SNe** i.e. WN stars (nitrogen dominating over carbon) exhibit the products of core-H burning. Alternatively, the outermost layers may be stripped off by a companion star (Podsiadlowski et al. 1992) with the degree of envelope-stripping depending on the configuration of the binary system (Pols & Nomoto 1997).

The distinction between type Ib and type Ic SNe is historical, and challenged by the idea that He may be present in both types.

The detection of spectral features due to He in type Ib SNe might simply imply that the element is high in abundance and/or a sufficient quantity of radioactive nickel is mixed into the He layer, providing an excitation source (Wheeler et al. 1987; Shigeyama et al. 1990; Hachisu et al. 1991). The converse may be true for type Ic SNe explaining the non-detection of optical He I lines in type Ic spectra (Nomoto et al. 1990; Hachisu et al. 1991). Most important, no type Ic SN has yet displayed the isolated near-IR He line at 2.058  $\mu\text{m}$  to a strength comparable to those detected in type Ib SNe.

Consequently, it is possible that a continuous degree of He abundances and/or excitation exists from type Ib to Ic SNe, making the



62 object names (412)

- 6-10 (1)
- C I (11)
- C II (3)
- DD-3 (1)
- GN-2007B (1)
- GN-2008B (1)
- H-K (1)
- 10830 (1)
- 15025 (1)
- 13888 (1)
- 15875 (1)
- 15876 (1)
- 15890 (1)
- 15896 (1)
- 16300 (1)
- 17774 (4)
- II 6355 (2)
- NGC 1058 (7)
- NGC 925 (2)
- P Cygni (5)
- Schaefer 1999 (1)
- Sep (4)
- SN 1961V (1)
- SN 1969L (1)
- SN 1983N (2)
- SN 1987A (14)
- SN 1990I (1)
- SN 1993J (1)
- SN 1994D (1)
- SN 1994I (27)
- SN 1995ad (1)
- SN 1997ef (1)
- SN 1998bw (10)
- SN 1998S (2)
- SN 1999em (2)
- SN 1999ex (5)
- SN 2000ew (3)
- SN 2001ig (1)
- SN 2002ap (49)
- SN 2003jd (6)
- SN 2004aw (15)
- SN 2004dj (4)
- SN 2004et (2)
- SN 2005af (1)
- SN 2005bf (1)
- SN 2006aj (4)
- SN 2007ar (159)

Fig. 7. Evolution of the optical spectra of **SN 2007gr**. The spectra have been corrected for reddening,  $E(B - V) = 0.092$ , and for the host galaxy redshift of **NGC 1058**,  $z = 0.001728$ . The spectra have also been magnified and displaced vertically for clarity by the numbers shown in brackets.

Identifications are shown in the spectra of **SN 2007gr** at

Fig. 8. Comparison of spectra of SNe close to B-band maximum (left) and at maximum light (right). All spectra are de-reddened and redshifted assuming the values reported in Table 2. Typical features are indicated by the numbers shown in brackets. The C I lines in the right-hand panel next to **SN 2007gr** indicate the positions of the C I lines. **SN 1994I** also shows a broad dip in this region; these variations are probably artefacts of the data reduction process. The O I lines in the right-hand panel next to **SN 2007gr** indicate the positions of the O I lines. The other SNe show a broad dip in this region; these variations are probably artefacts of the data reduction process.

Fig. 9. Comparison of spectra of SNe about one month (left) and about one month past maximum light (right). The O I lines in the right-hand panel next to **SN 2007gr** indicate the positions of the O I lines. The other SNe show a broad dip in this region; these variations are probably artefacts of the data reduction process.

Fig. 10. The Mg I]/[O I] ratio as a function of time for a sample of SNe. The Mg I] lines in the right-hand panel next to **SN 2007gr** indicate the positions of the Mg I] lines. The other SNe show a broad dip in this region; these variations are probably artefacts of the data reduction process.

Fig. 11. Left: the profiles of [O I] 6300, 6364 and Mg I] 4571 at +158 d past B maximum. The profile of [O I] is plotted in velocity space using a rest wavelength of 6315 Å, as obtained via Gaussian fitting from the modified profile of [O I] in the normal and low-density limits, 1:1, 3:1. The Mg I] profile includes the contribution of an artificial component with an intensity ratio of 1 and 0.33 (top and bottom panel, respectively) relative to the real peak and the same velocity offset as found in the oxygen doublet. The peaks of the Mg I] profiles have been scaled to match the peak of the oxygen doublet at +158 d. Centre: evolution of forbidden [O I] 5577, Mg I] 4571 and [O I] 6300, 6364. Right: evolution of the profiles of the permitted lines of O I] 7774 Å and Mg I] 7890 Å. The vertical line in the panels correspond to zero velocity i.e. the rest wavelengths of the line profiles.

Fig. 12. The near-infrared spectral evolution of **SN 2007gr**. The spectra are displayed in the rest frame of **NGC 1058**. To increase the temporal coverage we include the spectrum obtained by Valenti et al. (2008a) on day +15. The +376.6 d spectrum has been smoothed with a box size of 5 pixels. The spectra have been displaced vertically for clarity by the numbers shown in brackets. The rest wavelengths of possibly identified lines are also included.

Fig. 13. Comparison of the near-IR spectra of **SN 2007gr** to **SNe 2002ap** (broad-lined Ic), 1998bw (broad-lined Ic), 1999ex (type Ib), and 2004aw (type Ic). Note the presence of the prominent He I 1.083, and 2.0581 μm lines in the spectrum of **SN 1999ex**. See text for references.

Fig. 14. Evolution of the velocities from the different spectral lines observed in **SN 2007gr**. The errors in the measured velocities are estimated to be ~10%. The minimum error is not less than 500 km s<sup>-1</sup>.

Fig. 15. Comparison of the velocity evolution of the type Ic **SNe 2007gr**, **2004aw**, **2002ap**, and **1994I** using different spectral lines.

Fig. 16. Left: the CO emission profile of **SN 2007gr** (+137.7 d post B maximum) overlaid with the 192 d (post-explosion) spectrum of **SN 1987A**. The features indicated refer to **SN 1987A**. Right: CO profile of **SN 2007gr** at +137.7 d (post-B-maximum) overlaid with that of **SN 2004dj** at 137 d post-explosion.

Fe II

Acknowledgements. We would like to thank all the staff from the Asiago Ekar Telescope, Campo Imperatore Telescope, Calar Alto Observatory, Gemini North Telescope, Nordic Optical Telescope (operated on the island of La Palma jointly by Denmark, Finland, Iceland, Norway, and Sweden), Osservatorio di Teramo, Sternberg Astronomical Institute Telescope, Telescopio Nazionale Galileo, UKIRT, and the Wendelstein Telescope. The Gemini data reported here were obtained via programmes **GN-2007B-DD-3** and **GN-2008B-Q-58**.

We are grateful to the staff at the NOT: Amanda Djupvik, Thierry Morel, Jarkko Niemela, Tapio Pursimo, Auni Somero, John Telting and Helena Uthas, for observing **SN 2007gr**. We would also like to thank the staff at Gemini North: Thomas Dall, Tom Geballe, Silas Laycock, Atsuko Nitta, Kathy Roth, Ricardo Schiavon, Chad Trujillo and Kevin Volk, and also to the observers at the TNG: Avet Harutyunyan, Lorenzi Vania, and the Wendelstein observatory: Remus Bergemann, Florian Lang and Johannes Koppenhoefer.

L. Ryko acknowledges the Dark Cosmology Centre which is supported by the DNRF. R.K. and S.L.S. acknowledge financial support from STFC.

**Result**

Verification in Simbad:

existing names : 33  
not existing names : 29  
rejected occurrences : 20

Fig. 17. Evolution of the optical spectra of **SN 2007gr**. The spectra have been corrected for reddening,  $E(B - V) = 0.092$ , and for the host galaxy redshift of **NGC 1058**,  $z = 0.001728$ . The spectra have also been magnified and displaced vertically for clarity by the numbers shown in brackets.

Fig. 18. Comparison of spectra of SNe close to B-band maximum (left) and at maximum light (right). All spectra are de-reddened and redshifted assuming the values reported in Table 2. Typical features are indicated by the numbers shown in brackets. The C I lines in the right-hand panel next to **SN 2007gr** indicate the positions of the C I lines. **SN 1994I** also shows a broad dip in this region; these variations are probably artefacts of the data reduction process.

Fig. 19. Comparison of spectra of SNe about one month (left) and about one month past maximum light (right). The O I lines in the right-hand panel next to **SN 2007gr** indicate the positions of the O I lines. The other SNe show a broad dip in this region; these variations are probably artefacts of the data reduction process.

Fig. 20. The Mg I]/[O I] ratio as a function of time for a sample of SNe. The Mg I] lines in the right-hand panel next to **SN 2007gr** indicate the positions of the Mg I] lines. The other SNe show a broad dip in this region; these variations are probably artefacts of the data reduction process.

Fig. 21. Left: the profiles of [O I] 6300, 6364 and Mg I] 4571 at +158 d past B maximum. The profile of [O I] is plotted in velocity space using a rest wavelength of 6315 Å, as obtained via Gaussian fitting from the modified profile of [O I] in the normal and low-density limits, 1:1, 3:1. The Mg I] profile includes the contribution of an artificial component with an intensity ratio of 1 and 0.33 (top and bottom panel, respectively) relative to the real peak and the same velocity offset as found in the oxygen doublet. The peaks of the Mg I] profiles have been scaled to match the peak of the oxygen doublet at +158 d. Centre: evolution of forbidden [O I] 5577, Mg I] 4571 and [O I] 6300, 6364. Right: evolution of the profiles of the permitted lines of O I] 7774 Å and Mg I] 7890 Å. The vertical line in the panels correspond to zero velocity i.e. the rest wavelengths of the line profiles.

Fig. 22. The near-infrared spectral evolution of **SN 2007gr**. The spectra are displayed in the rest frame of **NGC 1058**. To increase the temporal coverage we include the spectrum obtained by Valenti et al. (2008a) on day +15. The +376.6 d spectrum has been smoothed with a box size of 5 pixels. The spectra have been displaced vertically for clarity by the numbers shown in brackets. The rest wavelengths of possibly identified lines are also included.

Fig. 23. Comparison of the near-IR spectra of **SN 2007gr** to **SNe 2002ap** (broad-lined Ic), 1998bw (broad-lined Ic), 1999ex (type Ib), and 2004aw (type Ic). Note the presence of the prominent He I 1.083, and 2.0581 μm lines in the spectrum of **SN 1999ex**. See text for references.

Fig. 24. Evolution of the velocities from the different spectral lines observed in **SN 2007gr**. The errors in the measured velocities are estimated to be ~10%. The minimum error is not less than 500 km s<sup>-1</sup>.

Fig. 25. Comparison of the velocity evolution of the type Ic **SNe 2007gr**, **2004aw**, **2002ap**, and **1994I** using different spectral lines.

Fig. 26. Left: the CO emission profile of **SN 2007gr** (+137.7 d post B maximum) overlaid with the 192 d (post-explosion) spectrum of **SN 1987A**. The features indicated refer to **SN 1987A**. Right: CO profile of **SN 2007gr** at +137.7 d (post-B-maximum) overlaid with that of **SN 2004dj** at 137 d post-explosion.

Fe II

Acknowledgements. We would like to thank all the staff from the Asiago Ekar Telescope, Campo Imperatore Telescope, Calar Alto Observatory, Gemini North Telescope, Nordic Optical Telescope (operated on the island of La Palma jointly by Denmark, Finland, Iceland, Norway, and Sweden), Osservatorio di Teramo, Sternberg Astronomical Institute Telescope, Telescopio Nazionale Galileo, UKIRT, and the Wendelstein Telescope. The Gemini data reported here were obtained via programmes **GN-2007B-DD-3** and **GN-2008B-Q-58**.

We are grateful to the staff at the NOT: Amanda Djupvik, Thierry Morel, Jarkko Niemela, Tapio Pursimo, Auni Somero, John Telting and Helena Uthas, for observing **SN 2007gr**. We would also like to thank the staff at Gemini North: Thomas Dall, Tom Geballe, Silas Laycock, Atsuko Nitta, Kathy Roth, Ricardo Schiavon, Chad Trujillo and Kevin Volk, and also to the observers at the TNG: Avet Harutyunyan, Lorenzi Vania, and the Wendelstein observatory: Remus Bergemann, Florian Lang and Johannes Koppenhoefer.

L. Ryko acknowledges the Dark Cosmology Centre which is supported by the DNRF. R.K. and S.L.S. acknowledge financial support from STFC.

- 62 object names (412)
- 6-10 (1)
- Text (1)
- 1
- CI (11)
- Text (9)
- Caption (2)
- CI II (3)
- Te
- Consequently, SN 2007gr was classified as a type Ic. Valenti et al. (2008a) studied the feature at 6450 Å, which may be misidentified as 6678 Å He I in early-time spectra, and suggest that a more plausible identification is C II 6580 Å at a velocity of ~11 000 km s. Indeed this feature disappears around maximum together with another feature at 7000 Å attributable to C II 7235 Å, thereby providing support for the Ic classification.
- DD-3
- GN-2
- GN-2008B (1)
- H-K (1)
- I 10830 (1)
- I 15025 (1)
- I 3888 (1)
- I 5875 (1)
- I 5876 (1)
- I 5890 (1)
- I 5896 (1)
- I 6300 (1)
- I 7774 (4)
- II 6355 (2)
- NGC 1058 (7)
- NGC 925 (2)
- P Cygni (5)
- Schaefer 1999 (1)
- Sep (4)
- SN 1961V (1)
- SN 1969L (1)
- SN 1983N (2)
- SN 1987A (14)
- SN 1990I (1)
- SN 1993J (1)
- SN 1994D (1)
- SN 1994I (27)
- SN 1995ad (1)
- SN 1997ef (1)
- SN 1998bw (10)
- SN 1998S (2)
- SN 1999em (2)
- SN 1999ex (5)
- SN 2000ew (3)
- SN 2001ig (1)
- SN 2002ap (49)
- SN 2003id (6)

# c(c) ESO 2009Astrophysics Extensive optical and near-infrared observations of the nearby, narrow-lined type Ic SN 2007gr: days 5 to 415\*

Text

D. I. Hunter, S. Valenti, R. Kotak, W. P. S. Meikle, S. Taubenberger, A. Pastorello, S. Benetti, V. Stanishev, S. J. Smartt, C. Trundle, A. A. Onov, P. Laursen, P. I.

## 1. Introduction

Text

One of the main objectives of supernovae (SNe) research is to understand the relation between the physics of the explosion and the nature of the progenitor star and its immediate environment.

Type I SNe, i.e. those lacking spectroscopic signatures of hydrogen, are divided into the Ia, Ib, and Ic categories. Of these, type Ia SNe constitute a physically distinct class and are believed to arise from the thermonuclear explosion of an accreting carbon-oxygen white dwarf. Instead, both the type Ib (He-rich) and the type Ic (He-poor) SNe are believed to originate from the core-collapse of stars more massive than ~8 M<sub>⊙</sub>.

SNe of type Ib and type Ic are quite heterogeneous in their spectral properties and energetics, which range from the relatively low kinetic energy (~10 erg) events like SN 1994I (Nomoto et al. 1994), to the high kinetic energy (~10 erg) broad-lined events sometimes dubbed "hypernovae" e.g. the broad-lined type Ic SNe 1998bw (Galama et al. 1998; Iwamoto et al. 1998) and 2003dh (Hjorth et al. 2003; Mazzali et al. 2003). These latter SNe have been associated with long-duration gamma-ray bursts (GRBs) (see Woosley & Bloom 2006, for a recent review).

At present, there is no consensus regarding the differences between the progenitors that produce type Ib and Ic SNe. However, it is generally accepted that Wolf-Rayet stars are the most promising candidates as these have shed their outer layer of H, as well as varying amounts of their He layer (Wheeler & Levreault 1985). The H and He layers are primarily shed through strong stellar winds, resulting in WC and WO stars (i.e. carbon and oxygen dominated, respectively). The same mass-loss mechanism may likewise only remove the H layers so that the potential progenitors of type Ib SNe i.e. WN stars (nitrogen dominating over carbon) exhibit the products of core-H burning. Alternatively, the outermost layers may be stripped off by a companion star (Podsiadlowski et al. 1992) with the degree of envelope-stripping depending on the configuration of the binary system (Pols & Nomoto 1997).

The distinction between type Ib and type Ic SNe is historical, and challenged by the idea that He may be present in both types. The detection of spectral features due to He in type Ib SNe might simply imply that the element is high in abundance and/or a sufficient quantity of radioactive nickel is mixed into the He layer, providing an excitation source (Wheeler et al. 1987; Shigeyama et al. 1990; Hachisu et al. 1991). The converse may be true for type Ic SNe explaining the non-detection of optical He I lines in type Ic spectra (Nomoto et al. 1990; Hachisu et al. 1991). Most importantly no type Ic SN has yet displayed the isolated near-IR He line at 2.058 μm to a strength comparable to those detected in type Ib SNe.

Consequently, it is possible that a continuous degree of He abundances and/or excitation exists from type Ib to Ic SNe, making the



Check found names Ctrl-N

Request SIMBAD

Request bibcode in SIMBAD

Search already entered names

Delete a name Supprimer

Mark selected names as done Ctrl-D

Mark selected names as undetermined Ctrl-Supprimer

View name list

Display rejected names...

Display undetermined names...

Display done names...

SN 1993J (1)

SN 1994D (1)

SN 1994I (27)

SN 1995ad (1)

SN 1997ef (1)

SN 1998bw (10)

SN 1998S (2)

SN 1999em (2)

SN 1999ex (5)

SN 2000ew (3)

SN 2001ig (1)

SN 2002ap (49)

SN 2003jd (6)

SN 2004aw (15)

SN 2004dj (4)

SN 2004et (2)

SN 2005af (1)

SN 2005bf (1)

SN 2006aj (4)

SN 2007gr (159)

SN 2008D (1)

SN 7 (1)

SN a (2)

SNe 1985F (2)

SNe 1987A (2)

SNe 1998bw (10)

SNe 1998dl (2)

SNe 2001ig (1)

SNe 2002ap (6)

SNe 2003jd (1)

SNe 2004aw (2)

SNe 2004dj (1)

SNe 2007gr (13)

SNe 2007Y (1)

SNe i (1)

: 508 Bibcode : 2009A&amp;A...508..371H

# astrophysics Extensive optical and near-infrared observations of low-lined type Ic SN 2007gr: days 5 to 415\*

W. P. S. Meikle, S. Taubenberger, A. Pastorello, S. Benetti, V. Stanishev, S. J. Smartt, C. Trundle, A. A. Arkharov, F. Carlo, M. Dolci, N. Elias-Rosa, S. Frandsen, J. U. Fynbo, U. Hopp, V. M. Larionov, P. Laursen, P. Mazzali, H. Navasardyan, D. Y. Tsvetkov, M. Turatto, and S. Wilke

## 1. Introduction

### Text

One of the main objectives of supernovae (SNe) research is to understand the relation between the physics of the explosion and the nature of the progenitor star and its immediate environment.

Type I SNe, i.e. those lacking spectroscopic signatures of hydrogen, are divided into the Ia, Ib, and Ic categories. Of these, type Ia SNe constitute a physically distinct class and are believed to arise from the thermonuclear explosion of an accreting carbon-oxygen white dwarf. Instead, both the type Ib (He-rich) and the type Ic (He-poor) SNe are believed to originate from the core-collapse of stars more massive than  $\sim 8 M_{\odot}$ .

SNe of type Ib and type Ic are quite heterogeneous in their spectral properties and energetics, which range from the relatively low kinetic energy ( $\sim 10$  erg) events like SN 1994H (Nomoto et al. 1994), to the high kinetic energy ( $\sim 10$  erg) broad-lined events sometimes dubbed "hypernovae" e.g. the broad-lined type Ic SNe 1998bw (Galama et al. 1998; Iwamoto et al. 1998) and 2003dh (Hjorth et al. 2003; Mazzali et al. 2003). These latter SNe have been associated with long-duration gamma-ray bursts (GRBs) (see Woosley & Bloom 2006, for a recent review).

At present, there is no consensus regarding the differences between the progenitors that produce type Ib and Ic SNe.

However, it is generally accepted that Wolf-Rayet stars are the most promising candidates as these have shed their outer layer of H, as well as varying amounts of their He layer (Wheeler & Levreault 1985). The H and He layers are primarily shed through strong stellar winds, resulting in WC and WO stars (i.e.

carbon and oxygen dominated, respectively). The same mass-loss mechanism may likewise only remove the H layers so that the potential progenitors of type Ib SNe, i.e. WN stars (nitrogen dominating over carbon) exhibit the products of core-H burning. Alternatively, the outermost layers may be stripped off by a companion star (Podsiadlowski et al. 1992) with the degree of envelope-stripping depending on the configuration of the binary system (Pols & Nomoto 1997).

The distinction between type Ib and type Ic SNe is historical, and challenged by the idea that He may be present in both types.

The detection of spectral features due to He in type Ib SNe might simply imply that the element is high in abundance and/or a sufficient quantity of radioactive nickel is mixed into the He layer, providing an excitation source (Wheeler et al. 1987; Shigeyama et al. 1990; Hachisu et al. 1991). The converse may be true for type Ic SNe explaining the non-detection of optical He I lines in type Ic spectra (Nomoto et al. 1990; Hachisu et al. 1991).

Most important, no type Ic SN has yet displayed the isolated near-IR He line at  $2.058 \mu\text{m}$  to a strength comparable to those detected in type Ib SNe. Consequently, it is possible that a continuous degree of He abundances and/or excitation exists from type Ib to Ic SNe, making the distribution smooth rather than bimodal. This seems consistent with the identification of intermediate cases such as SN 1998ex, which was characterised by weak optical He I lines, and strong He I  $\lambda 10830$ ,  $20581$  lines in the near-IR (Hamuy et al. 2002). Additionally, the transitional nature of SNe such as SN 2005bf (Folatelli et al. 2006) and SN 2008D (Soderberg et al. 2008; Mazzali et al. 2008; Malesani et al. 2009), both of which underwent a metamorphosis from a type Ic at early times to a type Ib at later epochs, may also provide an insight into the controversy of He. The current challenge lies in linking the observed variations of type Ib/c SNe to the physical properties of their progenitor systems.

This paper presents the results of an intensive observational follow-up campaign of the type Ic SN 2007gr from shortly after explosion to more than a year later. The layout of this paper is as follows: in Sect. 2 we provide some basic information on SN 2007gr and its host galaxy, with the data acquisition and reduction procedures described in Sect. 3. This is followed in Sect. 4 by a description of the optical and near-IR photometric behaviour, including the colour evolution and quasi-bolometric light curve. Section 5 is devoted to the spectroscopic evolution; we end with a summary in Sect. 6.

- 39 object names (365)
- NGC 1058 (7)
- NGC 925 (2)
- SN 1961V (1)
- SN 1969L (1)
- SN 1983N (2)
- SN 1987A (14)
- SN 1990I (1)
- SN 1993J (1)
- SN 1994D (1)
- SN 1994I (27)
- SN 1995ad (1)
- SN 1997ef (1)
- SN 1998bw (10)
- SN 1998S (2)
- SN 1999em (2)
- SN 1999ex (5)
- SN 2000ew (3)
- SN 2001ig (1)
- SN 2002ap (49)
- SN 2003jd (6)
- SN 2004aw (15)
- SN 2004dj (4)
- SN 2004et (2)
- SN 2005af (1)
- SN 2005bf (1)
- SN 2006aj (4)
- SN 2007gr (159)
- SN 2008D (1)
- SNe 1985F (2)
- SNe 1987A (2)
- SNe 1998bw (10)
- SNe 1998dl (2)
- SNe 2001ig (1)
- SNe 2002ap (6)
- SNe 2003jd (1)
- SNe 2004aw (2)
- SNe 2004dj (1)
- SNe 2007gr (13)
- SNe 2007Y (1)

# c(c) ESO 2009Astrophysics Extensive optical and near-infrared observations of the nearby, narrow-lined type Ic **SN 2007gr**: days 5 to 15\*

## Text

D. J. Hunter, S. Valenti, R. Kotak, W. P. S. Meikle, S. Taubenberger, A. Pastorello, S. Benetti, V. Stanishev, S. J. Smartt, C. Trundle, A. A. Arkharov, F. Bufano, E. Cappellaro, E. Di Carlo, M. Dolci, N. Elias-Rosa, S. Frandsen, J. U. Fynbo, U. Hopp, V. M. Larionov, P. Laursen, P. Mazzali, H. Navasardyan, C. Rie, A. Riffeser, L. Rizzi, D. Y. Tsvetkov, M. Turatto, and S. Wilke

## 1. Introduction

### Text

One of the main objectives of supernovae (SNe) research is to understand the relation between the physics of the explosion and the nature of the progenitor star and its immediate environment.

Type I SNe, i.e. those lacking spectroscopic signatures of hydrogen, are divided into the Ia, Ib, and Ic categories. Of these, type Ia SNe constitute a physically distinct class and are believed to arise from the thermonuclear explosion of an accreting carbon-oxygen white dwarf. Instead, both the type Ib (He-rich) and the type Ic (He-poor) SNe are believed to originate from the core-collapse of stars more massive than  $\sim 8 M_{\odot}$ .

SNe of type Ib and type Ic are quite heterogeneous in their spectral properties and energetics, which range from the relatively low kinetic energy ( $\sim 10$  erg) events like **SN 1994I** (Nomoto et al. 1994), to the high kinetic energy ( $\sim 10$  erg) broad-lined events sometimes dubbed "hypernovae" e.g. the broad-lined type Ic **SNe 1998bw** (Galama et al. 1998; Iwamoto et al. 1998) and **2003dt** (Hjorth et al. 2003; Mazzali et al. 2003). These latter SNe have been associated with long-duration gamma-ray bursts (GRBs) (see Woosley & Bloom 2006, for a recent review).

At present, there is no consensus regarding the differences between the progenitors that produce type Ib and Ic SNe. However, it is generally accepted that Wolf-Rayet stars are the most promising candidates as these have shed their outer layer of H, as well as varying amounts of their He layer (Wheeler & Levreault 1985). The H and He layers are primarily shed through strong stellar winds, resulting in WC and WO stars (i.e. carbon and oxygen dominated, respectively). The same mass-loss mechanism may likewise only remove the H layers so that the potential progenitors of type Ib SNe i.e. WN stars (nitrogen dominating over carbon) exhibit the products of core-H burning. Alternatively, the outermost layers may be stripped off by a companion star (Podsiadlowski et al. 1992) with the degree of envelope-stripping depending on the configuration of the binary system (Pols & Nomoto 1997).

The distinction between type Ib and type Ic SNe is historical, and challenged by the idea that He may be present in both types. The detection of spectral features due to He in type Ib SNe might simply imply that the element is high in abundance and/or a sufficient quantity of radioactive nickel is mixed into the He layer, providing an excitation source (Wheeler et al. 1987; Shigeyama et al. 1990; Hachisu et al. 1991). The converse may be true for type Ic SNe explaining the non-detection of optical He I lines in type Ic spectra (Nomoto et al. 1990; Hachisu et al. 1991). Most important, no type Ic SN has yet displayed the isolated near-IR He line at  $2.058 \mu\text{m}$  to a strength comparable to those detected in type Ib SNe. Consequently, it is possible that a continuous degree of He abundances and/or excitation exists from type Ib to Ic SNe, making the distribution smooth rather than bimodal. This seems consistent with the identification of intermediate cases such as **SN 1999ex**, which was characterised by weak optical He I lines, and strong He I  $\lambda\lambda 10830, 20581$  lines in the near-IR (Hamuy et al. 2002). Additionally, the transitional nature of SNe such as **SN 2005bf** (Folatelli et al. 2006) and **SN 2008S** (Soderberg et al. 2008; Mazzali et al. 2008; Malesani et al. 2009), both of which underwent a metamorphosis from a type Ic at early times to a type Ib at later epochs, may also provide an insight into the controversy of He. The current challenge lies in linking the observed variations of type Ib/c SNe to the physical properties of their progenitor systems.

This paper presents the results of an intensive observational follow-up campaign of the type Ic **SN 2007gr** from shortly after explosion to more than a year later. The layout of this paper is as follows: in Sect. 2 we provide some basic information on **SN 2007gr** and its host galaxy, with the data acquisition and reduction procedures described in Sect. 3. This is followed in Sect. 4 by a description of the optical and near-IR photometric behaviour, including the colour evolution and quasi-bolometric light curve. Section 5 is devoted to the spectroscopic evolution; we end with a summary in Sect. 6.

Journal : A&amp;A

Volume : 508

Bibcode : 2009A&amp;A...508..371H



39 object names (365)

- NGC 1058 (7)
- NGC 925 (2)
- SN 1961V (1)
- SN 1969L (1)
- SN 1983N (2)
- SN 1987A (14)
- SN 1990I (1)
- SN 1993J (1)
- SN 1994D (1)
- SN 1994I (27)
- SN 1995ad (1)
- SN 1997ef (1)
- SN 1998bw (10)
- SN 1998S (2)
- SN 1999em (2)
- SN 1999ex (5)
- SN 2000ew (3)
- SN 2001ig (1)
- SN 2002ap (49)
- SN 2003jd (6)
- SN 2004aw (15)
- SN 2004dj (4)
- SN 2004et (2)
- SN 2005af (1)
- SN 2005bf (1)
- SN 2006aj (4)
- SN 2007gr (159)
- SN 2008D (1)
- SNe 1985F (2)
- SNe 1987A (2)
- SNe 1998bw (10)
- SNe 1998dj (2)
- SNe 2001ig (1)
- SNe 2002ap (6)
- SNe 2003jd (1)
- SNe 2004aw (2)
- SNe 2004dj (1)
- SNe 2007gr (13)
- SNe 2007Y (1)

# c(c) ESO 2009Astrophysics Extensive optical and near-infrared observations of the nearby, narrow-lined type Ic **SN 2007gr**: days 5 to 415\*

## Text

D. J. Hunter, S. Valenti, R. Kotak, W. P. S. Meikle, S. Taubenberger, A. Pastorello, S. Benetti, V. Stanishev, S. J. Smartt, C. Trundle, A. A. Arkharov, F. Bufano, E. Cappellaro, E. Di Carlo, M. Dolci, N. Elias-Rosa, S. Frandsen, J. U. Fynbo, U. Hopp, V. M. Larionov, P. Laursen, P. Mazzali, H. Navasardyan, C. Rief, A. Riffeser, L. Rizzi, D. Y. Tsvetkov, M. Turatto, and S. Wilke

## 1. Introduction

### Text

One of the main objectives of supernovae (SNe) research is to understand the relation between the physics of the explosion and the nature of the progenitor star and its immediate environment.

Type I SNe, i.e. those lacking spectroscopic signatures of hydrogen, are divided into the Ia, Ib, and Ic categories. Of these, type Ia SNe constitute a physically distinct class and are believed to arise from the thermonuclear explosion of an accreting carbon-oxygen white dwarf. Instead, both the type Ib (He-rich) and the type Ic (He-poor) SNe are thought to be the result of the collapse of stars more massive than  $\sim 8 M_{\odot}$ .

SNe of type Ib and type Ic are quite heterogeneous. Type Ib SNe are typically associated with "broad-lined" events sometimes dubbed "hypernovae" e.g. the SN 1998bw (Nomoto et al. 1997) and SN 2003dh (Hjorth et al. 2003; Mazzali et al. 2003). These latter SNe have been associated with long-duration gamma-ray bursts (LIGO et al. 2006, for a recent review).

At present, there is no consensus regarding the exact nature of the progenitors that produce type Ib and Ic SNe. However, it is generally accepted that WC stars shed their outer layer of H, as well as varying amounts of their He layer (Wheeler & Levreault 1985). The H and He layers are primarily shed through strong stellar winds, resulting in WC and WO stars (i.e. carbon and oxygen dominated, respectively). The same mass-loss mechanism may likewise only remove the H layers so that the potential progenitors of type Ib SNe i.e. WN stars (nitrogen dominating over carbon) exhibit the products of core-H burning. Alternatively, the outermost layers may be stripped off by a companion star (Podsiadlowski et al. 1992) with the degree of envelope-stripping depending on the configuration of the binary system (Pols & Nomoto 1997).

The distinction between type Ib and type Ic SNe is historical, and challenged by the idea that He may be present in both types. The detection of spectral features due to He in type Ib SNe might simply imply that the element is high in abundance and/or a sufficient quantity of radioactive nickel is mixed into the He layer, providing an excitation source (Wheeler et al. 1987; Shigeyama et al. 1990; Hachisu et al. 1991). The converse may be true for type Ic SNe explaining the non-detection of optical He I lines in type Ic spectra (Nomoto et al. 1990; Hachisu et al. 1991). Most important, no type Ic SN has yet displayed the isolated near-IR He line at  $2.058 \mu\text{m}$  to a strength comparable to those detected in type Ib SNe. Consequently, it is possible that a continuous degree of He abundances and/or excitation exists from type Ib to Ic SNe, making the distribution smooth rather than bimodal. This seems consistent with the identification of intermediate cases such as SN 1999ex which was characterised by weak optical He I lines, and strong He I  $\lambda\lambda 10830, 20581$  lines in the near-IR (Hamuy et al. 2002). Additionally, the transitional nature of SNe such as SN 2005bf (Folatelli et al. 2006) and SN 2005E (Soderberg et al. 2008; Mazzali et al. 2008; Malesani et al. 2009), both of which underwent a metamorphosis from a type Ic at early times to a type Ib at later epochs, may also provide an insight into the controversy of He. The current challenge lies in linking the observed variations of type Ib/c SNe to the physical properties of their progenitor systems.

This paper presents the results of an intensive observational follow-up campaign of the type Ic SN 2007gr from shortly after explosion to more than a year later. The layout of this paper is as follows: in Sect. 2 we provide some basic information on SN 2007gr and its host galaxy, with the data acquisition and reduction procedures described in Sect. 3. This is followed in Sect. 4 by a description of the optical and near-IR photometric behaviour, including the colour evolution and quasi-bolometric light curve. Section 5 is devoted to the spectroscopic evolution; we end with a summary in Sect. 6.

Add a name

|                                    |                                   |
|------------------------------------|-----------------------------------|
| Simbad name :                      | Raw id :                          |
| SN 2003dh                          | 2003dh                            |
| <input type="button" value="Yes"/> | <input type="button" value="No"/> |

- 39 object names (365)
- NGC 1058 (7)
- NGC 925 (2)
- SN 1961V (1)
- SN 1969L (1)
- SN 1983N (2)
- SN 1987A (14)
- SN 1990I (1)
- SN 1993J (1)
- SN 1994D (1)
- SN 1994I (27)
- SN 1995ad (1)
- SN 1997ef (1)
- SN 1998bw (10)
- SN 1998S (2)
- SN 1999em (2)
- SN 1999ex (5)
- SN 2000ew (3)
- SN 2001ig (1)
- SN 2002ap (49)
- SN 2003jd (6)
- SN 2004aw (15)
- SN 2004dj (4)
- SN 2004et (2)
- SN 2005af (1)
- SN 2005bf (1)
- SN 2006aj (4)
- SN 2007gr (159)
- SN 2008D (1)
- SNe 1985F (2)
- SNe 1987A (2)
- SNe 1998bw (10)
- SNe 1998dl (2)
- SNe 2001ig (1)
- SNe 2002ap (6)
- SNe 2003jd (1)
- SNe 2004aw (2)
- SNe 2004dj (1)
- SNe 2007gr (13)
- SNe 2007Y (1)

maximum Epoch of  $-2.2 \pm 1.3$   $0 \pm 1.0$   $1.5 \pm 1.5$   $4.0 \pm 2.0$   $4.0 \pm 1.8$   $4.4 \pm 2.5$   $5.4 \pm 4.4$   $5.3 \pm 3.6$  maximum (days) Rising  $9.3 \pm 2.8$   $11.5 \pm 2.7$   $13.0 \pm 2.9$   $15.5 \pm 3.2$   $15.5 \pm 3.1$   $15.9 \pm 3.0$   $16.9 \pm 5.1$   $16.8 \pm 4.4$  times (days) Decline rates

Table 3

|            |                     |                     |                     |                     |                     |                     |                     |  |  |  |
|------------|---------------------|---------------------|---------------------|---------------------|---------------------|---------------------|---------------------|--|--|--|
| (30-100d)  | $0.0095 \pm 0.0007$ | $0.0111 \pm 0.0006$ | $0.0170 \pm 0.0005$ | $0.0194 \pm 0.0007$ | $0.0164 \pm 0.0004$ | $0.0304 \pm 0.0006$ | $0.0268 \pm 0.0008$ |  |  |  |
|            | $0.0342 \pm 0.0008$ |                     |                     |                     |                     |                     |                     |  |  |  |
| (100-170d) | $0.0169 \pm 0.0011$ | $0.0153 \pm 0.0003$ | $0.0189 \pm 0.0003$ | $0.0128 \pm 0.0004$ | $0.0167 \pm 0.0005$ |                     |                     |  |  |  |
| (30-170d)  | $0.0114 \pm 0.0006$ | $0.0130 \pm 0.0004$ | $0.0171 \pm 0.0003$ | $0.0159 \pm 0.0005$ | $0.0169 \pm 0.0002$ |                     |                     |  |  |  |

**Caption**

a A distance modulus  $\mu = 29.84 \pm 0.16$  mag and a colour excess  $E(B - V) = 0.092$  mag were adopted. The uncertainty in the epoch of maximum is defined as the time period in which the magnitude is not more than 0.01 mag fainter than the peak magnitude (Yoshii et al. 2003). Epoch with respect to the estimated B-band maximum JD 2 454 337.0  $\pm$  1.0. Epoch with respect to the estimated explosion date JD 2 454 325.5  $\pm$  2.5. e Decline rates (mag d) were estimated using linear least-square fitting.

Tab le 2. The parameters of type Ic SNe.

Table 4

| SN (Ic)                                      | Ni mass           | Ejecta mass | E <sub>v</sub> | m <sub>max</sub> | M <sub>max</sub> | Rise           | E(B - V) | $\mu$ | Redshift | Ref.           |
|--|-------------------|-------------|----------------|------------------|------------------|----------------|----------|-------|----------|----------------|
| (M <sub>v</sub> ) (M <sub>v</sub> ) (10 erg) | times (d)         |             |                |                  |                  |                |          |       |          |                |
| 2007gr                                       | $0.076 \pm 0.020$ | 2.0-3.5     | 1-4            | 13.47            | -16.75           | $11.5 \pm 2.5$ | 0.092    | 29.84 | 0.001728 | 1, 2           |
| 2004aw                                       | $0.30 \pm 0.05$   | 3.5-8.0     | 3.5-9.0        | 18.06            | -17.63           | .              | 0.370    | 34.17 | 0.015914 | 3              |
| 2003jd                                       | $0.36 \pm 0.04$   | 2.5-3.5     | 5-10           | 15.75            | -19.30           | ~13            | 0.144    | 34.46 | 0.018860 | 4              |
| 2002ap                                       | 0.09, 0.07        | 2.5-5.0     | 4-10           | 13.11            | -16.76           | ~8             | 0.090    | 29.50 | 0.002192 | 5, 6, 7, 8, 9  |
| 1998bw                                       | 0.7, 0.4, 0.5     | 10.9        | 20-50          | 14.09            | -18.44           | ~15            | 0.060    | 32.28 | 0.008670 | 10, 11, 12, 13 |
| 1997ef                                       | 0.13              | 9.6         | 17.5           | 17.45            | -16.18           | .              | 0.000    | 33.63 | 0.011688 | 14             |
| 1994I  | 0.07              | 0.88        | 1              | 13.77            | -17.06           | ~12            | 0.300    | 29.60 | 0.001544 | 15, 16, 17     |

**Caption**

References: Valenti et al. (2008a); this paper; Taubenberger et al. (2006); Valenti et al. (2008b); Yoshii et al. (2003); Foley et al. (2003); 7 Gal-Yam et al. (2002); Tomita et al. (2006); Mazzali et al. (2002); Iwamoto et al. (1998); Galama et al. (1998); Nakamura et al. (2001); 13 Patat et al. (2001); Mazzali et al. (2000); Nomoto et al. (1994); Richmond et al. (1996); Sauer et al. (2006). The peak absolute magnitudes were estimated using the apparent magnitudes at maxima. Total extinction. Redshift of the host galaxy (taken from the Nasa/IPAC Extragalactic Database NED).

Fig. 3. Optical light curves of SN 2007gr compared to those of the type Ic SNe 2004aw (Taubenberger et al. 2006), 2003jd (Valenti et al. 2008b), 2002ap (Pandey et al. 2003; Foley et al. 2003; Tomita et al. 2006), 1998bw (Galama et al. 1998; McKenzie & Schaefer 1999) and 1994I (Yo ko o et al. 1994; Gyoon et al. 1995; Lee et al. 1995; Tsvetkov & Pavlyuk 1995; Richmond et al. 1996). All the light curves presented have been shifted in time and magnitude to match SN 2007gr at maximum.

Fig. 4. The near-IR light curves of SNe 2007gr and 2002ap (Tomita et al. 2006). The filled symbols joined by the full lines represent the data for SN 2007gr. The data for SN 2002ap (open symbols, dotted lines) have been shifted in magnitude by 0.7, 0.7 and 0.5 mag to match SN 2007gr at ~20d in the JHK bands, respectively.

Fig. 5. Optical and near-infrared colour evolution of SN 2007gr compared with other SNe Ic: SN 2002ap, SN 2004aw, SN 1998bw, SN 1994I.

File Name Identifier Search Configuration Help

Search in the extracted text... Ctrl-F

New search with a prefix...

New search in a table...

Larger search...

Add a regular expression...

Remove a regular expression...

Table 3

07 0.0111 ± 0.0006 0.0170 ± 0.0005 0.0194 ± 0.0007 0.0164 ± 0.0004 0.0304 ± 0.0006 0.0268 ± 0.0008

08

(100-170d) 0.0111 ± 0.0006 0.0170 ± 0.0005 0.0194 ± 0.0007 0.0164 ± 0.0004 0.0304 ± 0.0006 0.0268 ± 0.0008

(30-170d) 0.0114 ± 0.0006 0.0130 ± 0.0004 0.0171

**Search in table**

Table number : from 4 to 4  
(The number shown in the extracted text and NOT from the original document)

Column number : 1

Prefix : SN

Select the whole column

OK Cancel

**Caption**

a A distance modulus  $\mu = 29.84 \pm 0.16$  mag and a colour defined as the time period in which the magnitude is not more than the estimated B-band maximum JD  $2\,454\,337.0 \pm 1.0$ . Epochs of maximum light (mag d) were estimated using linear least-squares fitting. Table 2. The parameters of type Ic SNe.

| SN (Ic)                                      | Ni mass       | Ejecta mass | E <sub>peak</sub> | Maximum light (mag d) | Maximum light (mag d) | Maximum light (mag d) | Maximum light (mag d) | Maximum light (mag d) | Maximum light (mag d) | Maximum light (mag d) | Maximum light (mag d) |
|--|---------------|-------------|-------------------|-----------------------|-----------------------|-----------------------|-----------------------|-----------------------|-----------------------|-----------------------|-----------------------|
| (M <sub>1</sub> ) (M <sub>2</sub> ) (10 erg) | times (d)     |             |                   |                       |                       |                       |                       |                       |                       |                       |                       |
| 2007gr                                       | 0.076 ± 0.020 | 2.0-3.5     | 1-4               | 13.47                 | -16.75                | 11.5 ± 2.5            | 0.092                 | 29.84                 | 0.001728              | 1, 2                  |                       |
| 2004aw                                       | 0.30 ± 0.05   | 3.5-8.0     | 3.5-9.0           | 18.06                 | -17.63                |                       | 0.370                 | 34.17                 | 0.015914              | 3                     |                       |
| 2003jd                                       | 0.36 ± 0.04   | 2.5-3.5     | 5-10              | 15.75                 | -19.30                | ~13                   | 0.144                 | 34.46                 | 0.018860              | 4                     |                       |
| 2002ap                                       | 0.09, 0.07    | 2.5-5.0     | 4-10              | 13.11                 | -16.76                | ~8                    | 0.090                 | 29.50                 | 0.002192              | 5, 6, 7, 8, 9         |                       |
| 1998bw                                       | 0.7, 0.4, 0.5 | 10.9        | 20-50             | 14.09                 | -18.44                | ~15                   | 0.060                 | 32.28                 | 0.008670              | 10, 11, 12, 13        |                       |
| 1997ef                                       | 0.13          | 9.6         | 17.5              | 17.45                 | -16.18                |                       | 0.000                 | 33.63                 | 0.011688              | 14                    |                       |
| 1994I  | 0.07          | 0.88        | 1                 | 13.77                 | -17.06                | ~12                   | 0.300                 | 29.60                 | 0.001544              | 15, 16, 17            |                       |

**Caption**

References: Valenti et al. (2008a); this paper; Taubenberger et al. (2006); Valenti et al. (2008b); Yoshii et al. (2003); Foley et al. (2003); Gal-Yam et al. (2002); Tomita et al. (2006); Mazzali et al. (2002); Iwamoto et al. (1998); Galama et al. (1998); Nakamura et al. (2001); Patat et al. (2001); Mazzali et al. (2000); Nomoto et al. (1994); Richmond et al. (1996); Sauer et al. (2006). The peak absolute magnitudes were estimated using the apparent magnitudes at maxima. Total extinction. Redshift of the host galaxy (taken from the Nasa/IPAC Extragalactic Database NED).

Fig. 3. Optical light curves of SN 2007gr compared to those of the type Ic SNe 2004aw (Taubenberger et al. 2006), 2003jd (Valenti et al. 2008b), 2002ap (Pandey et al. 2003; Foley et al. 2003; Tomita et al. 2006), 1998bw (Galama et al. 1998; McKenzie & Schaefer 1999) and 1994I (Yo ko o et al. 1994; Gyoon et al. 1995; Lee et al. 1995; Tsvetkov & Pavlyuk 1995; Richmond et al. 1996). All the light curves presented have been shifted in time and magnitude to match SN 2007gr at maximum.

Fig. 4. The near-IR light curves of SN 2007gr and 2002ap (Tomita et al. 2006). The filled symbols joined by the full lines represent the data for SN 2007gr. The data for SN 2002ap (open symbols, dotted lines) have been shifted in magnitude by 0.7, 0.7 and 0.5 mag to match SN 2007gr at ~20d in the JHK bands, respectively.

Fig. 5. Optical and near-infrared colour evolution of SN 2007gr compared with other SNe Ic: SN 2002ap, SN 2004aw, SN 1998bw, SN 1994I. Evolution of the U - B (top-left), B - V (top-middle), V - R (top-right), V - J (bottom-left), V - K (bottom-middle) and H - K (bottom-right) colours. The insets in two of the upper panels show a zoom-in of the early colour evolution of SN 2007gr compared to SN 2002ap. All curves have been corrected

- 39 object names (372)
- NGC 1058 (7)
- NGC 925 (2)
- SN 1961V (1)
- SN 1969L (1)
- SN 1983N (2)
- SN 1987A (14)
- SN 1990I (1)
- SN 1993J (1)
- SN 1994D (1)
- SN 1994I (28)
- SN 1995ad (1)
- SN 1997ef (2)
- SN 1998bw (11)
- SN 1998S (2)
- SN 1999em (2)
- SN 1999ex (5)
- SN 2000ew (3)
- SN 2001ig (1)
- SN 2002ap (50)
- SN 2003jd (7)
- SN 2004aw (16)
- SN 2004dj (4)
- SN 2004et (2)
- SN 2005af (1)
- SN 2005bf (1)
- SN 2006aj (4)
- SN 2007gr (160)
- SN 2008D (1)
- SNe 1985F (2)
- SNe 1987A (2)
- SNe 1998bw (10)
- SNe 1998dl (2)
- SNe 2001ig (1)
- SNe 2002ap (6)
- SNe 2003jd (1)
- SNe 2004aw (2)
- SNe 2004dj (1)
- SNe 2007gr (13)
- SNe 2007Y (1)

defined as the time period in which the magnitude is not more than 0.01 mag fainter than the peak magnitude (Yoshii et al. 2003). Epoch with respect to the estimated B-band maximum JD 2 454 337.0 ± 1.0. Epoch with respect to the estimated explosion date JD 2 454 325.5 ± 2.5. Decline rates (mag d) were estimated using linear least-square fitting.

Table 2. The parameters of type Ic SNe.

Table 4

| SN (Ic)                                      | Ni mass       | Ejecta mass | E <sub>v</sub> | m <sub>max</sub> | M <sub>max</sub> | Rise       | E(B - V) | mu    | Redshift | Ref.           |
|--|---------------|-------------|----------------|------------------|------------------|------------|----------|-------|----------|----------------|
| (M <sub>1</sub> ) (M <sub>2</sub> ) (10 erg) | times (d)     |             |                |                  |                  |            |          |       |          |                |
| 2007gr                                       | 0.076 ± 0.020 | 2.0-3.5     | 1-4            | 13.47            | -16.75           | 11.5 ± 2.5 | 0.092    | 29.84 | 0.001728 | 1, 2           |
| 2004aw                                       | 0.30 ± 0.05   | 3.5-8.0     | 3.5-9.0        | 18.06            | -17.63           |            | 0.370    | 34.17 | 0.015914 | 3              |
| 2003jd                                       | 0.36 ± 0.04   | 2.5-3.5     | 5-10           | 15.75            | -19.30           | ~13        | 0.144    | 34.46 | 0.018860 | 4              |
| 2002ap                                       | 0.09, 0.07    | 2.5-5.0     | 4-10           | 13.11            | -16.76           | ~8         | 0.090    | 29.50 | 0.002192 | 5, 6, 7, 8, 9  |
| 1998bw                                       | 0.7, 0.4, 0.5 | 10.9        | 20-50          | 14.09            | -18.44           | ~15        | 0.060    | 32.28 | 0.008670 | 10, 11, 12, 13 |
| 1997ef                                       | 0.13          | 9.6         | 17.5           | 17.45            | -16.18           |            | 0.000    | 33.63 | 0.011688 | 14             |
| 1994I  | 0.07          | 0.88        | 1              | 13.77            | -17.06           | ~12        | 0.300    | 29.60 | 0.001544 | 15, 16, 17     |

Caption

References: Valenti et al. (2008a); this paper; Taubenberger et al. (2006); Valenti et al. (2008b); Yoshii et al. (2003); Foley et al. (2003); 7 Gar-Yam et al. (2002); Tomita et al. (2006); Mazzali et al. (2002); Iwamoto et al. (1998); Galama et al. (1998); Nakamura et al. (2001); 13 Patat et al. (2001); Mazzali et al. (2000); Nomoto et al. (1994); Richmond et al. (1996); Sauer et al. (2006). The peak absolute magnitudes were estimated using the apparent magnitudes at maxima. Total extinction. Redshift of the host galaxy (taken from the Nasa/IPAC Extragalactic Database NED).

Fig. 3. Optical light curves of SN 2007gr compared to those of the type Ic SNe 2004aw, 2003jd (Taubenberger et al. 2006), 2002ap (Valenti et al. 2008b), 2002ap (Pandey et al. 2003; Foley et al. 2003; Tomita et al. 2006), 1998bw (Galama et al. 1998; McKenzie & Schaefer 1999) and 1994I (Yokoyama et al. 1994; Gyoon et al. 1995; Lee et al. 1995; Tsvetkov & Pavlyuk 1995; Richmond et al. 1996). All the light curves presented have been shifted in time and magnitude to match SN 2007gr at maximum.

Fig. 4. The near-IR light curves of SNe 2007gr and 2002ap (Tomita et al. 2006). The filled symbols joined by the full lines represent the data for SN 2007gr. The data for SN 2002ap (open symbols, dotted lines) have been shifted in magnitude by 0.7, 0.7 and 0.5 mag to match SN 2007gr at ~20d in the JHK bands, respectively.

Fig. 5. Optical and near-infrared colour evolution of SN 2007gr compared with other SNe Ic: SN 2002ap, SN 2004aw, SN 1998bw, SN 1994I. Evolution of the U - B (top-left), B - V (top-middle), V - R (top-right), V - J (bottom-left), V - K (bottom-middle) and H - K (bottom-right) colours. The insets in two of the upper panels show a zoom-in of the early colour evolution of SN 2007gr compared to SN 2002ap. All curves have been corrected for reddening. The Cardelli et al. (1989) law was used to estimate the extinction in the different bands. See text for references.

Fig. 6. The uvoir bolometric light curve of SN 2007gr and other type Ic SNe. The inset shows the differences in the widths of the uvoir lightcurves of this sample of type Ic SNe.

Fig. 7. Evolution of the optical spectra of SN 2007gr. The spectra have been corrected for reddening, E(B - V)<sub>0</sub> = 0.092, and for the host galaxy redshift of z = 0.001728. The spectra have also been magnified and displaced vertically for clarity by the numbers shown in brackets. Identifications are shown in the spectra of SN 2007gr at -6.5 and +158.4 days relative to B maximum.

Fig. 8. Comparison of spectra of SNe close to B-band maximum (left) and two-three weeks post maximum light (right). All spectra are de-reddened and redshifted assuming the values reported in Table 2. Typical absorption lines are identified. The three solid lines in the right-hand panel next to SN 2007gr indicate the positions of the C I lines. SN 1994I also shows the C I features, although these are not as strong as in SN 2007gr, while the other SNe show a broad dip in this region; these variations are probably attributable to the differences in the respective ejecta velocities of the SNe shown here, with the C I features being smeared out in those with the highest velocities.

- 39 object names (372)
- NGC 1058 (7)
- NGC 925 (2)
- SN 1961V (1)
- SN 1969L (1)
- SN 1983N (2)
- SN 1987A (14)
- SN 1990I (1)
- SN 1993J (1)
- SN 1994D (1)
- SN 1994I (28)
- SN 1995ad (1)
- SN 1997ef (2)
- SN 1998bw (11)
- SN 1998S (2)
- SN 1999em (2)
- SN 1999ex (5)
- SN 2000ew (3)
- SN 2001ig (1)
- SN 2002ap (50)
- SN 2003jd (7)
- SN 2004aw (16)
- SN 2004dj (4)
- SN 2004et (2)
- SN 2005af (1)
- SN 2005bf (1)
- SN 2006aj (4)
- SN 2007gr (160)
- SN 2008D (1)
- SNe 1985F (2)
- SNe 1987A (2)
- SNe 1998bw (10)
- SNe 1998dl (2)
- SNe 2001ig (1)
- SNe 2002ap (6)
- SNe 2003jd (1)
- SNe 2004aw (2)
- SNe 2004dj (1)
- SNe 2007gr (13)
- SNe 2007Y (1)

defined as the time period in which the magnitude is not more than 0.01 mag fainter than the peak magnitude (yosmi et al. 2003). Epoch with respect to the estimated B-band maximum JD 2 454 337.0 ± 1.0. Epoch with respect to the estimated explosion date JD 2 454 325.5 ± 2.5.

e Decline rate  
Table 2. T

31 identifiers (26 already entered)

|           |           |
|-----------|-----------|
| SN (c)    | NGC 1058  |
| (M_) (M_) | NGC 925   |
| 2007gr    | SN 1961V  |
| 2004aw    | SN 1969L  |
| 2003jd    | SN 1983N  |
| 2002ap    | SN 1987A  |
| 1998bw    | SN 1990I  |
| 1997ef    | SN 1993J  |
| 1994I     | SN 1994D  |
|           | SN 1994I  |
|           | SN 1995ad |
|           | SN 1997ef |
|           | SN 1998bw |
|           | SN 1998S  |
|           | SN 1999em |
|           | SN 1999ex |
|           | SN 2000ew |
|           | SN 2001ig |
|           | SN 2002ap |
|           | SN 2003jd |
|           | SN 2004aw |
|           | SN 2004dj |
|           | SN 2004et |
|           | SN 2005af |
|           | SN 2005bf |
|           | SN 2006aj |
|           | SN 2007gr |
|           | SN 2008D  |
|           | SN 1985F  |
|           | SN 1998dl |
|           | SN 2007Y  |

References:  
7 Gal-Yam  
13 Patat et  
estimated v  
NED).  
Fig. 3. Opti  
2002ap (Pa  
1994; Gyoc  
magnitude  
Fig. 4. The  
2007gr. Th  
the JHK bar  
Fig. 5. Opti  
Evolution o  
insets in tw  
for reddeni  
Fig. 6. The  
sample of t  
Fig. 7. Evolu  
of 2007gr  
Identificati

|                 |
|-----------------|
| Verify          |
| Visualize...    |
| Simulate        |
| Execute...      |
| Save as...      |
| Delete...       |
| Commands...     |
| from VizierR... |
| Coordinates...  |
| Properties...   |
| Duplicate       |
| Find/replace... |
| Close           |

| shift | Ref.           |
|-------|----------------|
| 01728 | 1, 2           |
| 5914  | 3              |
| 8860  | 4              |
| 02192 | 5, 6, 7, 8, 9  |
| 08670 | 10, 11, 12, 13 |
| 1688  | 14             |
| 01544 | 15, 16, 17     |

Fig. 8. Comparison of spectra of SNe close to B-band maximum (left) and two-three weeks post maximum light (right). All spectra are de-reddened and redshifted assuming the values reported in Table 2. Typical absorption lines are identified. The three solid lines in the right-hand panel next to SN 2007gr indicate the positions of the C I lines. SN 1994I also shows the C I features, although these are not as strong as in SN 2007gr, while the other SNe show a broad dip in this region; these variations are probably attributable to the differences in the respective ejecta velocities of the SNe shown here, with the C I features being smeared out in those with the highest velocities.

- 39 object names (372)
- NGC 1058 (7)
- NGC 925 (2)
- SN 1961V (1)
- SN 1969L (1)
- SN 1983N (2)
- SN 1987A (14)
- SN 1990I (1)
- SN 1993J (1)
- SN 1994D (1)
- SN 1994I (28)
- SN 1995ad (1)
- SN 1997ef (2)
- SN 1998bw (11)
- SN 1998S (2)
- SN 1999em (2)
- SN 1999ex (5)
- SN 2000ew (3)
- SN 2001ig (1)
- SN 2002ap (50)
- SN 2003jd (7)
- SN 2004aw (16)
- SN 2004dj (4)
- SN 2004et (2)
- SN 2005af (1)
- SN 2005bf (1)
- SN 2006aj (4)
- SN 2007gr (160)
- SN 2008D (1)
- SNe 1985F (2)
- SNe 1987A (2)
- SNe 1998bw (10)
- SNe 1998dl (2)
- SNe 2001ig (1)
- SNe 2002ap (6)
- SNe 2003jd (1)
- SNe 2004aw (2)
- SNe 2004dj (1)
- SNe 2007gr (13)
- SNe 2007Y (1)

defined as the time period in which the magnitude is not more than 0.01 mag fainter than the peak magnitude (Yosmii et al. 2003). Epoch with respect to the estimated B-band maximum JD 2 454 337.0 ± 1.0. Epoch with respect to the estimated explosion date JD 2 454 325.5 ± 2.5.

e Decline rate

Table 2. T

31 identifiers (26 already entered)

| SN (c)     | (M.) (M.) | Visualization |
|------------|-----------|---------------|
| NGC 1058   |           |               |
| NGC 925    |           |               |
| SN 1961V   |           |               |
| SN 1969L   |           |               |
| SN 1983N   |           |               |
| SN 1987A   |           |               |
| SN 1990I   |           |               |
| SN 1993J   |           |               |
| SN 1994D   |           |               |
| SN 1994I   |           |               |
| SN 1995ad  |           |               |
| SN 1997ef  |           |               |
| SN 1998bw  |           |               |
| SN 1998S   |           |               |
| SN 1999em  |           |               |
| SN 1999ex  |           |               |
| SN 2000ew  |           |               |
| SN 2001ig  |           |               |
| SN 2002ap  |           |               |
| SN 2003jd  |           |               |
| SN 2004aw  |           |               |
| SN 2004dj  |           |               |
| SN 2004et  |           |               |
| SN 2005af  |           |               |
| SN 2005bf  |           |               |
| SN 2006aj  |           |               |
| SN 2007gr  |           |               |
| SN 2008D   |           |               |
| SNe 1985F  |           |               |
| SNe 1987A  |           |               |
| SNe 1998bw |           |               |
| SNe 1998dl |           |               |
| SNe 2001ig |           |               |
| SNe 2002ap |           |               |
| SNe 2003jd |           |               |
| SNe 2004aw |           |               |
| SNe 2004dj |           |               |
| SNe 2007gr |           |               |
| SNe 2007Y  |           |               |

References:

7 Gal-Yam

13 Patat et

estimated v

NED).

Fig. 3. Opti

2002ap (Pa

1994; Gyoc

magnitude

Fig. 4. The

SN 2003jd (1)

the JHK bar

Fig. 5. Opti

Evolution o

insets in tw

for reddeni

Fig. 6. The

sample of t

Fig. 7. Evolu

of

Identificati

SN 1994I

o SN 1983N, +x, +SN 1983N, = 2

SN 200

o SN 1987A, +xg, +SN 1987A; SNe 1987A, = 16

SN 200

o SN 1990I, +x, +SN 1990I, = 1

SN 200

o SN 1993J, +c, +SN 1993J, = 1

SN 200

o SN 1994D, +x, +SN 1994D, = 1

SN 199

o SN 1994I, +xcd, +SN 1994I, = 28

2007gr

o SN 1995ad, +x, +SN 1995ad, = 1

v

o SN 1997ef, +xd, +SN 1997ef, = 2

v

Close

| shift | Ref.           |
|-------|----------------|
| 01728 | 1, 2           |
| 5914  | 3              |
| 8860  | 4              |
| 02192 | 5, 6, 7, 8, 9  |
| 08670 | 10, 11, 12, 13 |
| 1688  | 14             |
| 01544 | 15, 16, 17     |

Status processed  Question  Raw idents  Bibcode

Fig. 8. Comparison of spectra of SNe close to B-band maximum (left) and two-three weeks post maximum light (right). All spectra are de-reddened and redshifted assuming the values reported in Table 2. Typical absorption lines are identified. The three solid lines in the right-hand panel next to SN 2007gr indicate the positions of the C I lines. SN 1994I also shows the C I features, although these are not as strong as in SN 2007gr, while the other SNe show a broad dip in this region; these variations are probably attributable to the differences in the respective ejecta velocities of the SNe shown here, with the C I features being smeared out in those with the highest velocities.



## *Updating SIMBAD*

---

- ★ Automatically check for different names for the same object
- ★ Display additional information (raw identifier, number of occurrences, positions in the text)
- ★ Commands can be added to each identifier to add data
- ★ VizieR could be queried to look into large surveys (ex: 2MASS, USNO, ...)
- ★ After check, the command files are automatically created, they can be simulated, displayed, saved, edited



## *After 2 years of usage*

---

- ★ A very deep change in the way people work
- ★ Visual tool,  
Efficient for easy object names, lists, ... ← avoid bothersome work  
Concentrated the work on added value aspects
- ★ Time saved for a some types of papers (theoretical, ...)
- ★ Still need human checking with a very good knowledge of astronomy to :
  - avoid wrong detections
  - detect new identifiers
  - detect what is not highlighted



Mission

[SSC2008]

TABLE 2  
 Chandra X-RAY SOURCES IN THE VICINITY OF  $\sigma$  ORI AB

2MASS

| CXO Number            | R.A.<br>(J2000.0) | Decl.<br>(J2000.0) | Net Counts      | $\langle E \rangle$<br>(keV) | $K_s$<br>(mag) | J                      | Identification (Offset<br>1 (arcsec)) |
|-----------------------|-------------------|--------------------|-----------------|------------------------------|----------------|------------------------|---------------------------------------|
| 1.....                | 05 38 29.12       | -02 36 03.0        | 69 ± 8 (v.99)   | 1.58                         | 11.69          | 2M 053829.12-023602.7  | (0.30)                                |
| 2.....                | 05 38 31.43       | -02 36 33.8        | 7 ± 3           | 1.29                         | 10.99          | 2M 053831.41-023633.8  | (0.24)                                |
| 3.....                | 05 38 31.57       | -02 35 14.7        | 32 ± 6          | 2.07                         | 10.35          | 2M 053831.58-023514.9  | (0.24)                                |
| 4.....                | 05 38 32.83       | -02 35 39.4        | 147 ± 12        | 1.35                         | 10.73          | 2M 053832.84-023539.2  | (0.30)                                |
| 5.....                | 05 38 33.34       | -02 36 18.3        | 21 ± 5          | 1.41                         | 11.11          | 2M 053833.36-023617.6  | (0.72)                                |
| 6.....                | 05 38 34.04       | -02 36 37.2        | 8 ± 3           | 1.10                         | 11.08          | 2M 053834.06-023637.5  | (0.42)                                |
| 7.....                | 05 38 34.31       | -02 35 00.2        | 50 ± 7          | 1.29                         | 10.35          | 2M 053834.31-023500.1  | (0.12)                                |
| 8.....                | 05 38 35.21       | -02 34 38.1        | 369 ± 19 (v.95) | 3.01                         | ...            | M07:053835.22-023438.0 | (0.18)                                |
| 9.....                | 05 38 38.22       | -02 36 38.6        | 390 ± 20 (v.99) | 1.79                         | 10.31          | 2M 053838.22-023638.4  | (0.18)                                |
| 10.....               | 05 38 38.48       | -02 34 55.2        | 697 ± 26 (v.97) | 1.60                         | 9.12           | 2M 053838.49-023455.0  | (0.24)                                |
| 11.....               | 05 38 39.72       | -02 40 19.2        | 12 ± 4 (v.96)   | 3.09                         | 12.88          | 2M 053839.73-024019.7  | (0.54)                                |
| 12.....               | 05 38 41.21       | -02 37 37.4        | 29 ± 5          | 3.40                         | 14.04          | 2M 053841.23-023737.7  | (0.48)                                |
| 13.....               | 05 38 41.28       | -02 37 22.7        | 323 ± 18        | 1.64                         | 10.59          | 2M 053841.29-023722.6  | (0.24)                                |
| 14.....               | 05 38 41.35       | -02 36 44.6        | 14 ± 4          | 1.13                         | 12.08          | 2M 053841.35-023644.5  | (0.12)                                |
| 15.....               | 05 38 42.27       | -02 37 14.5        | 9 ± 3           | 2.56                         | 10.77          | 2M 053842.28-023714.7  | (0.30)                                |
| 16.....               | 05 38 43.01       | -02 36 14.7        | 6 ± 3           | 1.93                         | 10.63          | 2M 053843.02-023614.6  | (0.18)                                |
| 17.....               | 05 38 43.85       | -02 37 07.3        | 16 ± 4          | 1.38                         | 11.77          | 2M 053843.87-023706.9  | (0.54)                                |
| 18.....               | 05 38 44.22       | -02 40 20.0        | 158 ± 13        | 1.52                         | 10.44          | 2M 053844.23-024019.7  | (0.30)                                |
| 19.....               | 05 38 44.76       | -02 36 00.3        | 2514 ± 50       | 0.86                         | 4.49           | 2M 053844.76-023600.2  | (0.12); $\sigma$ Ori AB               |
| 20.....               | 05 38 44.83       | -02 35 57.4        | 43 ± 7 (v.95)   | 1.37                         | ...            | $\sigma$ Ori IRS 1     |                                       |
| 21.....               | 05 38 45.35       | -02 41 59.6        | 50 ± 5          | 1.69                         | 11.04          | 2M 053845.37-024159.4  | (0.42)                                |
| 22 <sup>a</sup> ..... | 05 38 46.82       | -02 36 43.5        | 6 ± 2           | 0.95                         | 12.35          | 2M 053846.85-023643.5  | (0.48)                                |
| 23.....               | 05 38 47.19       | -02 35 40.5        | 454 ± 21 (v.98) | 1.56                         | 6.95           | 2M 053847.20-023540.5  | (0.18); $\sigma$ Ori E                |
| 24.....               | 05 38 47.46       | -02 35 25.4        | 87 ± 9          | 1.64                         | 10.72          | 2M 053847.46-023525.3  | (0.18)                                |
| 25.....               | 05 38 47.89       | -02 37 19.6        | 188 ± 14 (v.99) | 2.20                         | 10.78          | 2M 053847.92-023719.2  | (0.54)                                |
| 26.....               | 05 38 48.27       | -02 36 41.2        | 42 ± 7          | 1.35                         | 11.14          | 2M 053848.29-023641.0  | (0.30)                                |
| 27.....               | 05 38 48.68       | -02 36 16.4        | 106 ± 10 (v.95) | 1.35                         | 11.17          | 2M 053848.68-023616.2  | (0.18)                                |
| 28.....               | 05 38 49.12       | -02 41 23.9        | 22 ± 6          | 1.62                         | ...            | S04:053849.14-024124.8 | (0.96)                                |
| 29.....               | 05 38 49.17       | -02 38 22.5        | 112 ± 11        | 1.32                         | 10.51          | 2M 053849.17-023822.2  | (0.24)                                |



[MNL SJ]

[FPS2006] NX 99

annot.pdf - Adobe Reader  
File Edit View Document Tools Window Help  
annot.pdf x

NOTES.—Units of right ascension are hours, minutes, and seconds, and units of declination are degrees, arcminutes, and arcseconds. X-ray data are from CCD-7 (ACIS chip S3) using events in the 0.5–7 keV range. Tabulated quantities are running source number, X-ray position (R.A., decl.), net counts and net counts error from *wavdetect* (accumulated in a 90,967 s exposure, rounded to the nearest integer, background subtracted, and PSF corrected), mean photon energy ( $\langle E \rangle$ ),  $K_s$  magnitude of near-IR 2MASS counterpart, and 2MASS (2M) or optical (S04; M07 = Mayne et al. 2007) candidate counterpart identification within a  $2''$  search radius. The offset (arcseconds) between the X-ray and counterpart position is given in parentheses. A (v) following net counts error indicates that the source is likely variable as indicated by a variability probability  $P_{\text{var}} \geq 0.95$  determined from the K-S statistic. The number following v is the K-S variability probability, i.e., v.99 indicates a variability probability  $P_{\text{var}} = 0.99$ . All sources were confirmed to be present in the archived 98 ks *Chandra* HRC-I image (ObsID 2560).

<sup>a</sup> Low-significance *wavdetect* detection ( $2 < \text{significance} < 3$ ).

<sup>b</sup> Probable *XMM-Newton* counterpart is source NX 99 in Table B.1 of FPS06. High value of  $\langle E \rangle$  suggests possible extragalactic background source.

<sup>c</sup> Double star with a B5 V primary and a companion at separation  $0.45''$  (Caballero 2005).

which have high cluster membership probability (92%–93%). Their mass estimates from S04 are  $0.22 M_{\odot}$  (S04 15) and  $0.18 M_{\odot}$  (S04 18), and their respective  $V - R_c$  colors imply equivalent main-sequence spectral types of  $\sim M4 V$ – $M5 V$  (Kenyon & Hartmann 1995). Also noteworthy is *Chandra* source CXO 22, which was classified as M5 by FPS06 but was listed in their Table A2 (object name B3.01-67) as undetected by *XMM-Newton*.

Some of the faint sources in Table 2 are likely extragalactic background objects. In particular, the five sources without optical or near-IR identifications are extragalactic candidates since

all are faint ( $\leq 25$  counts), nonvariable, and have above average mean photon energies. If we assume a typical extragalactic source power-law X-ray spectrum with a photon power-law index  $\Gamma = 1.4$ ,  $N_H = 3 \times 10^{20} \text{ cm}^{-2}$ , and a 7 count detection threshold, then the hard-band (2–8 keV) number counts from the Chandra Deep Field-North (CDF-N) observations (Cowie et al. 2002) predict  $\approx 15$  extragalactic sources in the ACIS-S3 CCD field of view above our detection limit. The expression for hard-band (2–8 keV) number counts obtained from CDF-N data by Brandt et al. (2001) gives a similar result. However, the accuracy of the  $\log N - \log S$

8.50 x 11.25 in

[SWW2004] J053650.626-021858.39

[SWW2004] J053700.310-022826.34

[SSC2008] 22

[KJN2005] 3,01-67

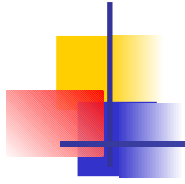
NAME CDF-N



# *Statistics*

---

- ★ Rate of exact recognition : 75%
- ★ Rate of partial recognition : 12% ← new acronyms
- ★ Rate of missing recognition : 10% ← tables, figures, ...
- ★ Rate of false detections : 3 %
- ★ Rate of noise : 51% ← choice for this application
  
- ★ Saving time ?



## *Other Applications*

---

- ★ According the object's position in the article and its occurrence, after checking everything, it is possible to identify the most important papers for one object.

## References (3029 between 2000 and 2010)

Simbad bibliographic survey began in 1950 for stars (at least bright stars) and in 1983 for all other objects (outside the solar system).

display

reference summary

When available, the bibcode is followed by ***the status of the object*** in the reference

from: 2000 to: 2010

[2010AJ...139...59B](#) [ x , 1 ]

Astron. J., 139, 59-67 (2010)

**Velocity dispersion profile of the Milky Way halo**

BROWN W.R., GELLER M.J., KENYON S.J. and DIAFERIO A.

**Comments & notes:**

**CDS status:** *waiting for electronic table*

**flags:** (abstract)

[2010AJ...139..372C](#) [ t k a x c , 55 ]

Astron. J., 139, 372-377 (2010)

**A star in the M31 giant stream: the highest negative stellar velocity known.**

CALDWELL N., MORRISON H., KENYON S.J., SCHIAVON R., HARDING P. and ROSE J.A.

**Comments & notes:**

**flags:** (abstract)

[2010ApJ...708..293Y](#) [ a x , 6 ]

Astrophys. J., 708, 293-303 (2010)

**RR Lyrae variables in the Local Group dwarf galaxy NGC 147.**

YANG S.-C. and SARAJEDINI A.

**Comments & notes:**

**flags:** (abstract)

[2010ApJ...708..817F](#) [ k a x c f , 61 ]

Astrophys. J., 708, 817-833 (2010)

**RR Lyrae variables in M32 and the disk of M31.**

FIorentino G., MONACHESI A., TRAGER S.C., LAUER T.R., SAHA A., MIGHELL K.J., FREEDMAN W., DRESSLER A., GRILLMAIR C. and TOLSTOY E.

**Comments & notes:**

**flags:** (abstract)

[2010ApJ...708.1076T](#) [ x c f , 3 ]

Astrophys. J., 708, 1076-1091 (2010)

**The WHIQII survey: metallicities and spectroscopic properties of luminous compact blue galaxies.**

TOLLERUD E.J., BARTON E.J., VAN ZEE L. and COOKE J.

**Comments & notes:**

**CDS status:** *waiting for electronic table*

**flags:** (abstract)

[2010ApJ...708.1168T](#) [ t k a s x c d , 170 ]

Astrophys. J., 708, 1168-1203 (2010)

**Structure and population of the Andromeda stellar halo from a Subaru/Suprime-Cam survey.**

TANAKA M., CHIBA M., KOMIYAMA Y., GUHATHAKURTA P., KALIRAI J.S. and IYE M.

**Comments & notes:**

**flags:** (abstract)

[2010ApJ...708.1290C](#) [ x , 1 ]

Astrophys. J., 708, 1290-1309 (2010)

**A two micron all sky survey view of the Sagittarius dwarf galaxy. VI. s-process and titanium abundance variations along the**

The tags defining the status of an object in its reference are:

- t : the object is in the title
- a : the object is cited in the abstract
- k : the object appears in the keyword list
- s : the object appears in a subtitle
- c : the object is cited in a caption
- d : the object is listed in a table
- f : the object is in a figure
- x : the object is in the text of the paper
- o : the object is defined in a object tag
- z : the object is implicitly defined in the paper
- \* : the object is cited as a calibrator

The list of tags may be followed by the number of occurrences of the object in the article.



## *Other Applications*

---

- ★ According the object's position in the article and its occurrence, after checking everything, it is possible to identify the most important papers for one object.
- ★ Links between SIMBAD <-> NED  
NED shares the information about nomenclature

SIMBAD query result - Mozilla Firefox

Fichier Édition Affichage Historique Marque-pages Outils Aide

http://simbad.u-strasbg.fr/simbad/sim-id?ident=M+31&Nbident=1&Radius=2&Radius.ur

radius  arcmin



---

**References (5880 between 1850 and 2010)**  
*Simbad bibliographic survey began in 1950 for stars (at least bright stars) and in 1983 for all other objects (outside the solar system).*

display  
reference summary

from:  to:

---

**Measurements (9 types) :**

distance : 1    IRAS : 1    IRC : 1    ISO : 156    IUE : 13    posa : 1    RVel : 4    XMM : 22    ze : 1

display selected measurements   display all measurements   clear

---

**External archives :**

Archive data at [HEASARC - High-Energy Astrophysics Science Archive Research Center](#)

Data at [NED - NASA/IPAC Extragalactic Database](#)

Catalogue information from [VizieR](#)

[IRAS F00400+4059](#)   [IRAS 00400+4059](#)   [IRC +40013](#)   [2MASX J00424433+4116074](#)   [NGC 224](#)  
[RAFG1 104](#)   [UGC 454](#)

---

**Annotations :**

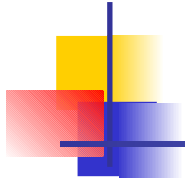
Currently no annotations available

[add an annotation](#)

---

To bookmark this query, right click on this link: [simbad:M 31](#) and select 'bookmark this link' or equivalent in the popup menu

©UDS/CNRS Contact: 



# LISA VI

---

## DJIN : Detection in Journals of Identifiers and Names

*by Soizick Lesteven*

*C. Bonnin, S. Derrière, P. Dubois, F. Genova, A. Oberto, F. Ochsenbein, S. Borde, G. Chassagnard,  
M. Brouty, C. Bruneau, C. Brunet, H. Claude, A. Eisele, S. Laloë, M. Neuville, E. Perret, P. Vannier,  
P. Vonflie, M.-J. Wagner and F. Woelfel*

*Pune 2010*